



Article scientifique

Article

2015

Published version

Open Access

This is the published version of the publication, made available in accordance with the publisher's policy.

Hepatic PTEN deficiency improves muscle insulin sensitivity and decreases adiposity in mice

Peyrou, Marion; Bourgoïn, Lucie; Poher, Anne-Laure; Altirriba Gutierrez, Jorge; Maeder Garavaglia, Christine; Caillon, Aurélie; Fournier, Margot; Montet, Xavier Cédric Rodolphe; Rohner-Jeanraud, Françoise; Foti, Michelangelo

How to cite

PEYROU, Marion et al. Hepatic PTEN deficiency improves muscle insulin sensitivity and decreases adiposity in mice. In: Journal of hepatology, 2015, vol. 62, n° 2, p. 421–429. doi: 10.1016/j.jhep.2014.09.012

This publication URL: <https://archive-ouverte.unige.ch/unige:47591>

Publication DOI: [10.1016/j.jhep.2014.09.012](https://doi.org/10.1016/j.jhep.2014.09.012)

Hepatic *PTEN* deficiency improves muscle insulin sensitivity and decreases adiposity in mice

Marion Peyrou^{1,†}, Lucie Bourgoïn^{1,†}, Anne-Laure Poher², Jordi Altirriba², Christine Maeder¹, Aurélie Caillon², Margot Fournier¹, Xavier Montet³, Françoise Rohner-Jeanrenaud², Michelangelo Foti^{1,*}

¹Department of Cellular Physiology and Metabolism, Faculty of Medicine, University of Geneva, Switzerland; ²Department of Internal Medicine Specialties, Division of Endocrinology, Diabetology, Hypertension and Nutrition, Faculty of Medicine, University of Geneva, Switzerland; ³Department of Radiology, Faculty of Medicine, University of Geneva, Switzerland

Background & Aims: *PTEN* is a dual lipid/protein phosphatase, downregulated in steatotic livers with obesity or HCV infection. Liver-specific *PTEN* knockout (*LPTEN* KO) mice develop steatosis, inflammation/fibrosis and hepatocellular carcinoma with aging, but surprisingly also enhanced glucose tolerance. This study aimed at understanding the mechanisms by which hepatic *PTEN* deficiency improves glucose tolerance, while promoting fatty liver diseases.

Methods: Control and *LPTEN* KO mice underwent glucose/pyruvate tolerance tests and euglycemic-hyperinsulinemic clamps. Body fat distribution was assessed by EchoMRI, CT-scan and dissection analyses. Primary/cultured hepatocytes and insulin-sensitive tissues were analysed *ex vivo*.

Results: *PTEN* deficiency in hepatocytes led to steatosis through increased fatty acid (FA) uptake and *de novo* lipogenesis. Although *LPTEN* KO mice exhibited hepatic steatosis, they displayed increased skeletal muscle insulin sensitivity and glucose uptake, as assessed by euglycemic-hyperinsulinemic clamps. Surprisingly, white adipose tissue (WAT) depots were also drastically reduced. Analyses of key enzymes involved in lipid metabolism further indicated that FA synthesis/esterification was decreased in WAT. In addition, *Ucp1* expression and multilocular lipid droplet structures were observed in this tissue, indicating the presence of beige adipocytes. Consistent with a liver to muscle/adipocyte crosstalk, the expression of liver-derived circulating factors, known to impact on muscle insulin sensitivity and WAT homeostasis (e.g. FGF21), was modulated in *LPTEN* KO mice.

Conclusions: Although steatosis develops in *LPTEN* KO mice, *PTEN* deficiency in hepatocytes promotes a crosstalk between liver and muscle, as well as adipose tissue, resulting in enhanced insulin sensitivity, improved glucose tolerance and decreased adiposity.

© 2014 European Association for the Study of the Liver. Published by Elsevier B.V. All rights reserved.

Introduction

Non-alcoholic fatty liver disease (NAFLD) encompasses a spectrum of liver metabolic disorders, starting with an excessive accumulation of neutral lipids in cytoplasmic droplets of hepatocytes (steatosis), which can then progress towards inflammation, fibrosis and cirrhosis. Obesity and viral infections are common causes of these chronic liver diseases, which are often accompanied by insulin resistance (IR). Indeed, lipotoxicity, resulting from excessive overloading of hepatocytes with lipids, was reported to affect insulin-stimulated signalling pathways that control glucose and lipid metabolism [1]. Hepatic IR is likely to represent a precursor event, leading to systemic and long-standing IR [2]. Uncontrolled hepatic glucose output may indeed induce hyperglycemia and compensatory hyperinsulinemia, favouring IR development in other organs. In turn, insulin-resistant muscle and adipose tissue exacerbate hepatic metabolic disorders, thus nourishing a vicious circle of peripheral IR. Lipotoxicity, inflammation and systemic IR contribute with time to the alteration of pancreatic β -cell function and survival, resulting in their inability to secrete enough insulin to counteract peripheral tissues IR, therefore leading to the development of type 2 diabetes [2,3]. In turn, diabetes favours steatosis evolution towards steatohepatitis, fibrosis/cirrhosis and hepatocellular carcinoma, again creating a vicious circle [4].

Insulin signalling is highly regulated at different levels by multiple mechanisms. Among them, the phosphatase and tensin homolog (*PTEN*) is a dual specificity protein and phosphoinositide phosphatase that dephosphorylates $\text{PtdIns}(3,4,5)\text{P}_3$, the product of PI3K [5]. By metabolizing $\text{PtdIns}(3,4,5)\text{P}_3$, *PTEN* interrupts insulin signalling downstream of PI3K. This *PTEN* antagonistic effect on PI3K signalling [6] and its nuclear function

Keywords: Steatosis; Beige adipocyte; Glucose tolerance; Gluconeogenesis; Organ crosstalk; FGF21.

Received 26 March 2014; received in revised form 3 September 2014; accepted 9 September 2014

* Corresponding author. Address: Department of Cell Physiology and Metabolism, CMU, 1 rue Michel-Servet, 1211 Geneva 4, Switzerland. Tel.: +41 22 3795204; fax: +41 22 3795260.

E-mail address: Michelangelo.foti@unige.ch (M. Foti).

[†] These authors contributed equally to this work.

Abbreviations: *PTEN*, phosphatase and tensin homolog; *LPTEN* KO, liver-specific *PTEN* knockout mice; WAT, white adipose tissue; FA, fatty acid; NAFLD, non-alcoholic fatty liver disease; IR, insulin resistance; GTT, glucose tolerance test; PTT, pyruvate tolerance test; TG, triglyceride; NEFA, non-esterified fatty acid; UCP1, uncoupling protein 1; FGF21, fibroblast growth factor 21.



ELSEVIER

Journal of Hepatology 2014 vol. xxx | xxx-xxx

Research Article

on chromosomal stability [7] position PTEN as an important tumour suppressor, which is often deleted/mutated or downregulated in human cancers [6].

Alterations of PTEN expression/activity are also expected to deeply affect lipid and glucose homeostasis. Indeed, *PTEN* heterozygosity and *PTEN* tissue-specific deletions in muscle or adipose tissue all lead to improved glucose tolerance in healthy or obese/diabetic mice [8–10]. However, adding to the complexity of PTEN function, transgenic mice, overexpressing PTEN, display increased energy expenditure and insulin sensitivity [11,12]. Regarding the liver, we previously reported that PTEN is downregulated in steatotic livers of obese patients, as well as in rat models of genetic or diet-induced obesity [13]. Likewise, PTEN is downregulated in the liver of patients infected with hepatitis C virus (HCV) [14]. Interestingly, both obesity and HCV infection are associated with the development of steatosis and IR. However, liver-specific *PTEN* knockout mice (*LPTEN* KO) exhibit an ambiguous phenotype. Indeed, *LPTEN* KO mice develop sequentially hepatic steatosis, inflammation/fibrosis and hepatocellular carcinoma with aging, indicating that PTEN plays a crucial role in the development of these pathologies [15,16]. Yet, *LPTEN* KO mice also exhibit an improved glucose tolerance, which is unexpected with NAFLD [15,16]. This study aimed at understanding the mechanisms through which liver-specific *PTEN* deficiency improves glucose tolerance, while promoting NAFLD.

Materials and methods

Reagents, antibodies, and cell cultures

All reagents, antibodies, commercial kits, cell isolation and cell culture are described in the [Supplementary Materials and methods](#) section.

Animals

Pten^{flox/flox} (CTL) and *AlbCre-Pten*^{flox/flox} (*LPTEN* KO) mice generated as previously described [15], were housed at 23 °C; light cycle: 07.00 am–07.00 pm and had free access to water and standard diet. All experiments were conducted in accordance with the Swiss guidelines for animal experimentation and were ethically approved by the Geneva Health head office. 4-month old mice were sacrificed using isoflurane anaesthesia followed by rapid decapitation and blood/tissues were collected and stored at –80 °C.

Metabolic phenotyping, EchoMRI, and CT-scan

Energy expenditure and the respiratory exchange ratio were determined by indirect calorimetry: locomotor activity was recorded by an infrared frame, and food and fluid intake were measured by highly sensitive feeding and drinking sensors. These parameters were measured in mice housed individually in Labmaster metabolic cages (TSE, Bad Homburg, Germany) after 5 days of adaptation prior to recording. Fuel (carbohydrate plus protein vs. fat) oxidation was calculated as described by Bruss *et al.* [17]. An EchoMRI-700 quantitative nuclear magnetic resonance analyzer (Echo Medical Systems, Houston, TX) was used to measure total fat and lean mass. Distribution, volume and weight of fat depots were analysed by a multidetector CT-scan (Discovery 750 HD, GE Healthcare, Milwaukee, USA) and dissection after sacrifice. For cold exposure, mice were housed in a 6 °C cold room up to 24 h and body temperature was measured at the indicated time points.

Glucose, pyruvate tolerance tests (GTT, PTT) and insulin injections

After overnight starvation, mice were administered intraperitoneally with glucose (1.5 g.kg⁻¹) or pyruvate (2 g.kg⁻¹) and glycaemia was measured from tail blood during 2 h. To investigate insulin signalling in organs, mice were injected intraperitoneally with 150 mU/g of insulin (or PBS) 40 min before sacrifice, as previously validated [18].

Euglycemic-hyperinsulinemic clamps

4 h fasted mice were anesthetized with intraperitoneal pentobarbital (80 mg.kg⁻¹). As previously described [19], euglycemic-hyperinsulinemic clamps were performed, using insulin infusion at a dose suppressing hepatic glucose production (18 mU.kg⁻¹.min⁻¹), and the glucose infusion rate was measured. At steady state, a bolus of 2-deoxy-D-(1-³H)glucose (30 µCi) was injected to determine the *in vivo* glucose utilization index of insulin-sensitive tissues. 2-deoxy-D-(1-³H)glucose-6-phosphate in peripheral tissues was measured using a liquid scintillation analyzer (Tri-Carb 2900TR, Perkinelmer, MA, USA).

Histological analyses

Tissues were fixed in 4% paraformaldehyde and 6 µm thin sections were stained with haematoxylin/eosin for morphological investigations. Quantifications were performed using the Metamorph software.

Plasma and tissue analyses

Plasma triglycerides (TGs) were determined by an automated Abott Architect analyzer (Abott Architect, Paris, France). Plasma glucose, insulin, non-esterified fatty acids (NEFA), lactate, ketone bodies and FGF21 levels, as well as liver content of TGs, glycogen and ketone bodies were measured with commercial kits.

Real-time PCR

RNA was extracted using Trizol according to the manufacturer's instructions. 1 µg of RNA was reverse transcribed using a VILO kit. Quantitative RT-PCRs were performed using a SYBR green detector on a StepOne PCR system (Life Technologies, Carlsbad, USA). Primer sequences are listed in [Supplementary Table 1](#).

Western blot analyses

Homogenized cells/tissues were lysed in ice-cold RIPA buffer. Proteins were resolved by 5–20% gradient SDS-PAGE and blotted onto nitrocellulose membranes. Proteins were detected with specific primary antibodies and HRP-conjugated secondary antibodies using chemoluminescence. Quantifications were performed using the ChemiDoc™ XRS from Biorad (Cressier, Switzerland) and the Quantity One™ Software.

Statistical analysis

Results are expressed as means ± SEM of at least 3 independent experiments or at least 4 different animals per group. Results were analysed by Student's *t* test or two-way ANOVA followed by a Sidak's multiple comparisons test when more than 2 groups or multiple time points were analysed. Values were considered significant when **p* < 0.05, ***p* < 0.01 or ****p* < 0.001.

Results

Hepatic steatosis in *LPTEN* KO mice is associated with increased glycolysis but decreased gluconeogenesis and glucose output

As previously reported, *LPTEN* KO mice have an increased liver weight related to triglyceride (TG) accumulation in hepatocytes ([Supplementary Fig. 1](#) and [16]). We found two mechanisms contributing to excessive TG accumulation in the liver of *LPTEN* KO mice. First, mRNA expression levels of FA transporters, in particular *Cd36*, *Fatp3*, and *Fabp1*, were significantly upregulated, suggesting increased FA uptake from the bloodstream by *PTEN*-deficient hepatocytes ([Supplementary Fig. 2](#)). Secondly, critical effectors promoting *de novo* lipogenesis were strongly overexpressed in the liver of *LPTEN* KO mice. In particular, the mRNA expression of *Fas*, *Acc1*, *Acc2*, *Scd1*, *Pparγ*, and *Srebp1c* was upregulated. In addition, protein expression of key enzymes involved in

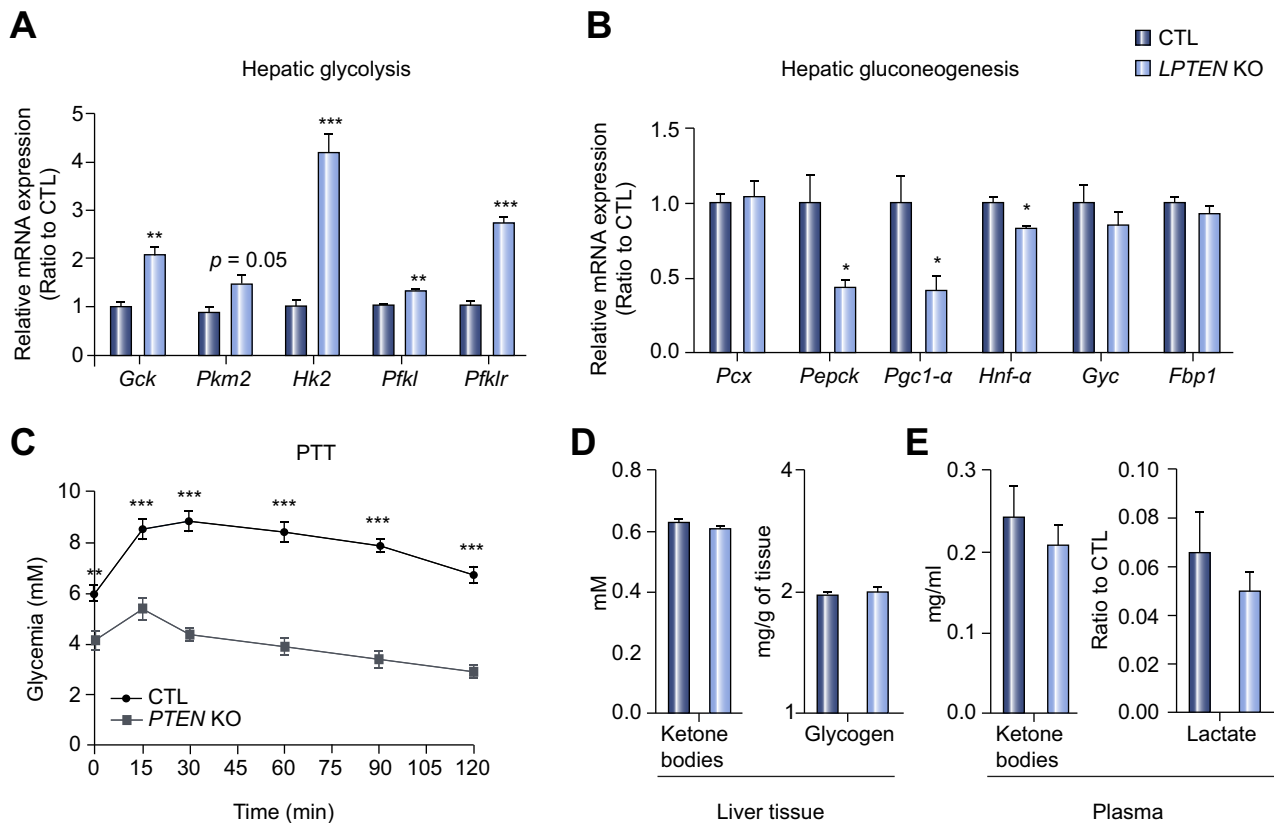


Fig. 1. Increased hepatic glycolysis and decreased gluconeogenesis in *LPTEN* KO mice. Relative mRNA expression of genes involved in hepatic glycolysis (A) and gluconeogenesis (B). (C) Pyruvate tolerance test after overnight fasting. (D) Ketone bodies and glycogen levels in liver tissue. (E) Ketone bodies and lactate levels in plasma. Values are mean \pm SEM of at least 4 animals per group.

FA biosynthesis, i.e. FA synthase (FAS) and acetyl-CoA carboxylase (ACC), was also strongly increased in *PTEN*-depleted hepatic tissue. On the contrary, the general expression pattern of rate-limiting key enzymes controlling hepatic FA oxidation, lipolysis and export, as well as cholesterol metabolism, mainly remained unchanged with the exception of a few enzymes weakly up- or downregulated (Supplementary Fig. 2).

Hepatic steatosis is usually tightly associated with IR [20]. However, glucose tolerance tests (GTT) indicated that *LPTEN* KO mice paradoxically exhibited an improved glucose tolerance associated with hypoinsulinemia (Supplementary Fig. 1C and D). The liver appeared to contribute in two ways to this improved glucose tolerance of *LPTEN* KO mice. Consistent with a boosted *de novo* lipogenesis (Supplementary Fig. 2), glucose utilization was strongly promoted, as indicated by an increased mRNA expression of enzymes regulating glycolysis (Fig. 1A). Secondly, the mRNA expression of key factors promoting gluconeogenesis, i.e. *Pepck* and *Pgc1-α*, was downregulated in *LPTEN* KO mice, suggesting an impairment of *de novo* glucose synthesis (Fig. 1B). This was further confirmed by pyruvate tolerance tests (PTTs), showing that the pyruvate-dependent hepatic glucose output was strongly abrogated in *LPTEN* KO mice (Fig. 1C). Although *de novo* glucose production was inhibited in *LPTEN* KO mice, we did not observe any changes, neither in the liver glycogen content, nor in ketone bodies, which can arise from increased pyruvate production through the glycolytic oxidative pathway. Plasma lactate levels remained unchanged as well (Fig. 1D and E).

These results indicate that FA synthesis is fostered by an increase in glucose utilization, whereas inhibition of gluconeogenesis and glucose output contributes to the improved glucose tolerance in *LPTEN* KO mice.

LPTEN KO mice display enhanced systemic insulin sensitivity and insulin-stimulated glucose uptake in skeletal muscle

Although impaired hepatic gluconeogenesis and glucose output likely contribute to the improved glucose tolerance of *LPTEN* KO mice, insulin sensitivity and glucose uptake by peripheral organs, i.e. skeletal muscle and adipose tissues, are also important potential mechanisms to be considered. To address this issue, we first examined the phosphorylation/activation of AKT, a major insulin signalling effector, in peripheral organs of *LPTEN* KO vs. CTL mice injected with insulin. As shown in Fig. 2A, *LPTEN* KO mice, stimulated with insulin, displayed lower activation of the insulin receptor (INSR) in the liver, but higher basal and insulin-stimulated AKT phosphorylation, due to a lack of the PTEN antagonistic effect on PI3K signalling. Surprisingly, although PTEN expression was not altered in non-hepatic and metabolically active tissues of *LPTEN* KO mice (Supplementary Fig. 1E and F) and despite the presence of higher TG levels in muscle (Supplementary Fig. 5), phosphorylation of the INSR and its downstream effector, AKT, was significantly increased in muscles of *LPTEN* KO mice, indicating muscle insulin hypersensitivity (Fig. 2B). Contrasting with skeletal muscle, AKT phosphorylation in white adipose tissue

Research Article

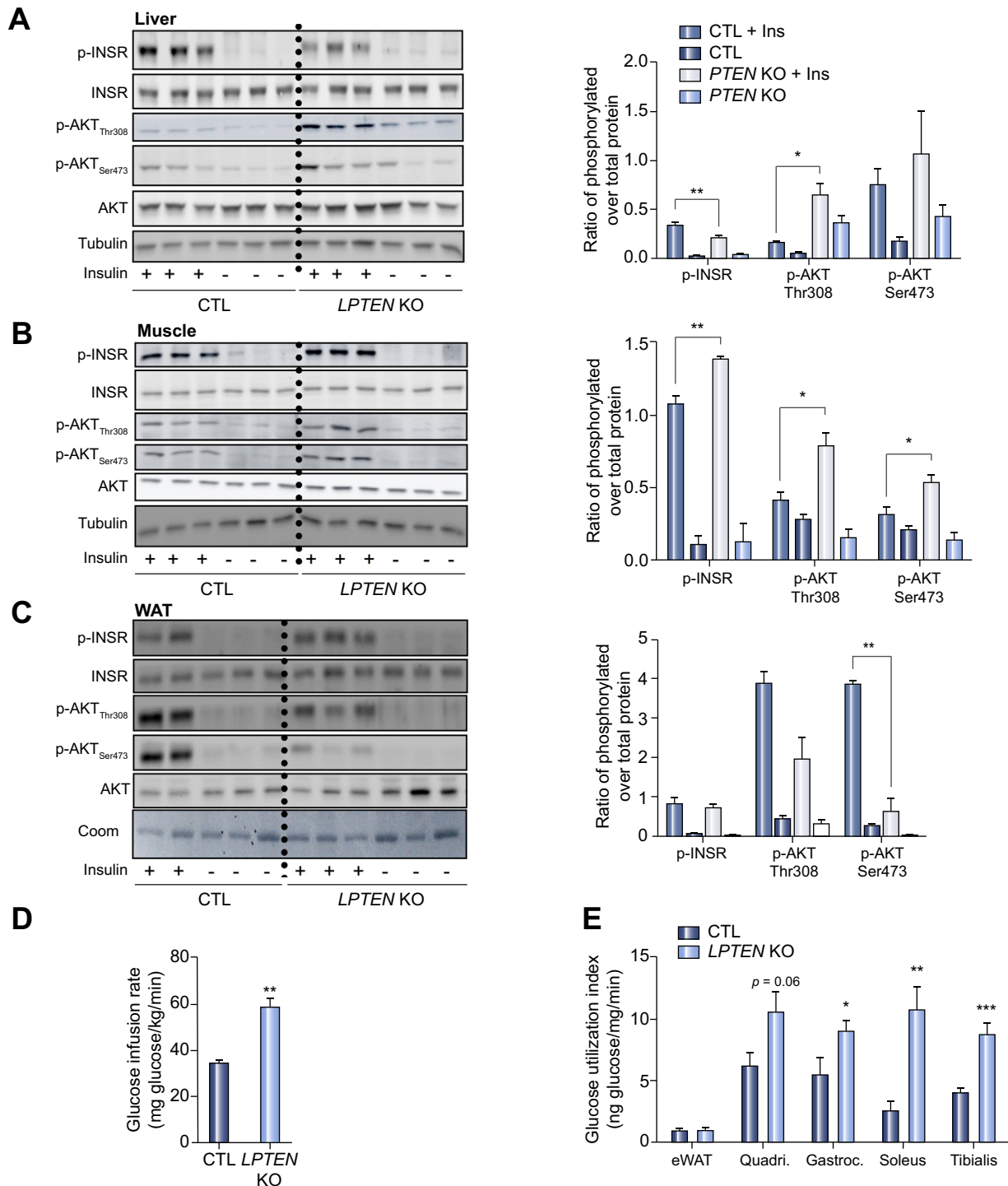


Fig. 2. Enhanced insulin sensitivity and insulin-stimulated glucose uptake in skeletal muscles of *LPTEN* KO mice. Representative Western blots and quantification of phosphorylated over total protein levels of insulin effectors in the liver (A), muscle (soleus) (B) and WAT (epididymal) (C) after overnight fasting and injection of insulin (150 mU/g) or PBS 40 min before sacrifice. (D) Glucose infusion rate during euglycemic-hyperinsulinemic clamps. (E) Glucose utilization index measured in epididymal WAT and skeletal muscle (quadriceps, gastrocnemius, soleus and tibialis). Values are mean \pm SEM of 3 (A–C) and 6 for (D–E) animals per group.

(WAT) of *LPTEN* KO mice was reduced, although INSR phosphorylation was unaffected (Fig. 2C).

To further evaluate the influence of skeletal muscle on the glucose tolerance of *LPTEN* KO mice, we performed

euglycemic-hyperinsulinemic clamps under conditions of complete suppression of hepatic glucose production. We observed that the glucose infusion rate (GIR) measured at the end of the clamps was highly increased in *LPTEN* KO mice, confirming

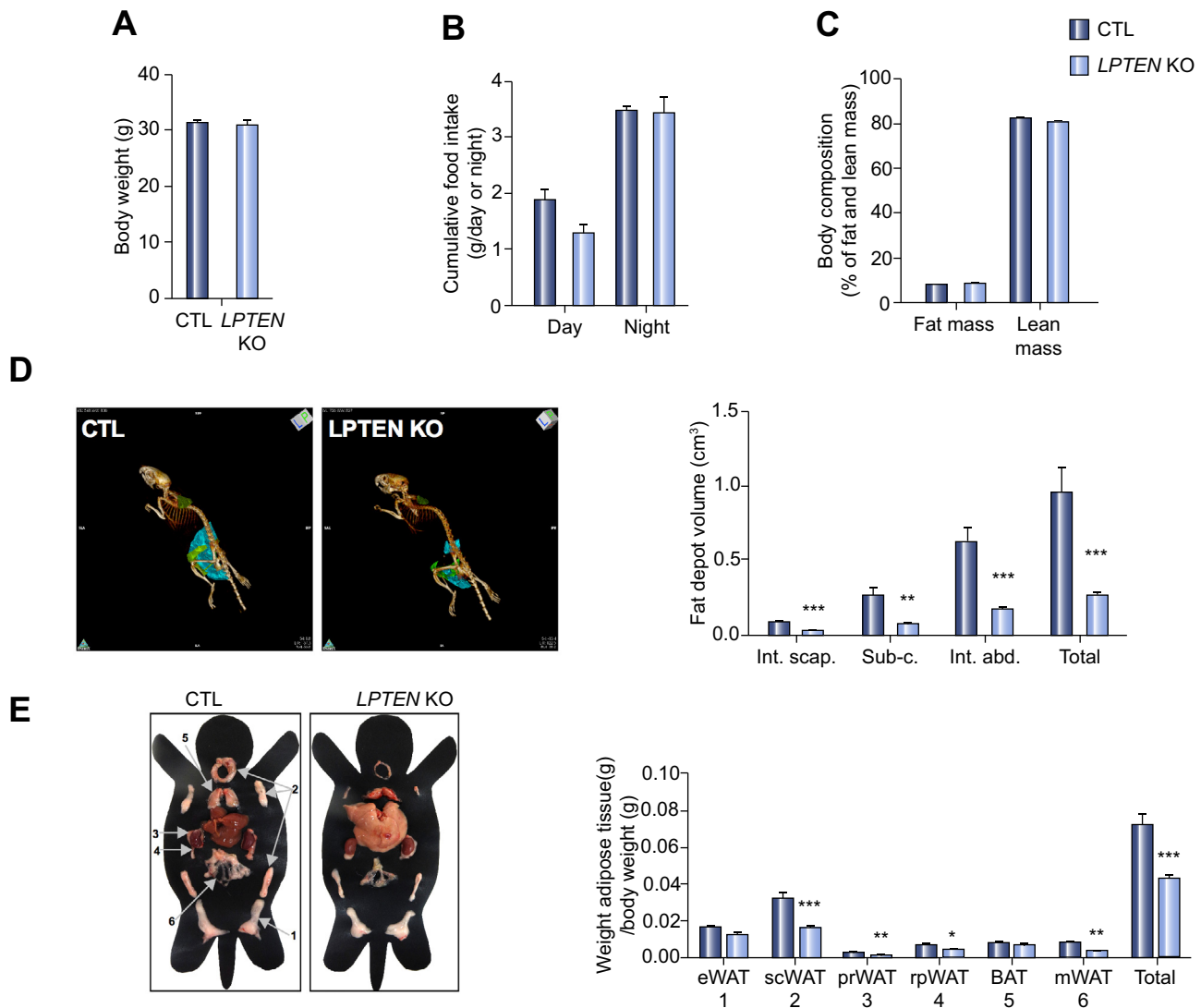


Fig. 3. Decreased lipid storage in white adipose depots of *LPTEN* KO mice. (A) Total body weight. (B) Cumulative food intake. (C) Percentage of total fat and lean body mass measured by EchoMRI. (D) Localization and volumes of fat depots measured by CT-scan. Interscapular brown/white adipose tissue depots (Int. scap., green), subcutaneous WAT (Sub-c, light green), intra-abdominal WAT (Int abd., turquoise). (E) Weights of white adipose tissue (WAT): eWAT, epididymal; scWAT, sub-cutaneous; prWAT, perirenal; rpWAT, retro-peritoneal; mWAT, mesenteric) and brown adipose tissue (BAT) depots. Values are mean \pm SEM of at least 4 animals per group.

enhanced peripheral insulin sensitivity (Fig. 2D). Consistent with this observation, insulin-induced glucose uptake was increased in almost all skeletal muscle types examined, while it remained unaffected in WAT (Fig. 2E).

These results indicate that hepatic *PTEN*-deficiency induces muscle insulin hypersensitivity, which importantly contributes to the improved glucose tolerance observed in *LPTEN* KO mice.

Hepatic *PTEN* deletion decreases lipid storage in fat depots

Analysis of the overall phenotypic characteristics of *LPTEN* KO mice showed that their body weight and food intake were unaltered compared to CTL mice (Fig. 3A and B). The same was also the case for locomotor activity, energy expenditure and the respiratory exchange ratio (RER) measured by indirect calorimetry, as well as thermal regulation upon cold exposure (Supplementary Fig. 3). Furthermore, when body composition was assessed by

EchoMRI analysis, the total lean and fat mass remained similar in both groups (Fig. 3C). However, *LPTEN* KO mice exhibited marked hepatic steatosis, as previously reported (Supplementary Fig. 1 and [16]). In view of these results, the normal overall fat content of *LPTEN* KO mice suggested a decrease in adipose tissue depots. We therefore used quantitative CT-scan imaging to measure fat depot volumes. Data obtained indicated that the volumes of interscapular, subcutaneous and intraperitoneal WAT depots were drastically reduced in *LPTEN* KO mice (Fig. 3D). This was further confirmed by accurate dissection and weighing of all visible fat depots in CTL and *LPTEN* KO mice (Fig. 3E). On the contrary, the volume and weight of major brown adipose tissue depots (e.g. interscapular) were unchanged in *LPTEN* KO as compared to CTL mice.

We then analysed the mRNA expression of major effectors involved in lipid metabolism of mesenteric WAT (a representative WAT in the context of metabolic diseases) and did not detect

Research Article

any important and significant change in the expression of key enzymes regulating FA uptake or lipolysis (Supplementary Fig. 4A and C), consistent with the absence of significant changes in plasma TG and non-esterified fatty acid (NEFA) levels (Supplementary Fig. 5A). Although the RER (ratio of VCO_2/VO_2) tended to decrease and fat oxidation to increase (Supplementary Fig. 3C and D) during the diurnal period, the expression of critical rate-limiting enzymes, controlling fatty acid β -oxidation, was not significantly altered (Supplementary Fig. 4C). However, Western blot analyses of FAS and ACC, two major enzymes required for FA biosynthesis, revealed a decrease in the expression of these proteins in WAT of *LPTEN* KO mice with no change in their respective mRNAs (Supplementary Fig. 4B). Reduction in FA esterification was also suggested by a decreased mRNA expression of *Gpat1* (Supplementary Fig. 4A).

Together, these data indicate that *PTEN*-deficiency in the liver decreases adiposity through crosstalk mechanisms between the liver and WAT, preventing FA synthesis and esterification in WAT.

Browning of mesenteric WAT occurs in LPTEN KO mice and correlates with increased FGF21 production and release by the liver

Recent evidence indicates that browning of WAT (appearance of brown-like adipocytes called "beige cells" in WAT) may also importantly contribute to a decreased adiposity and improved metabolic status in mice [21]. Beige cells with high FA oxidation capacity in WAT are differentiated from classical white adipocytes by mainly two specific characteristics: (i) the expression of the uncoupling protein *Ucp1* and (ii) multilocular lipid droplet structures, instead of a single large lipid droplet [21]. As shown in Fig. 4A, *Ucp1* expression was increased in specific WAT depots of *LPTEN* KO mice, such as the mesenteric depot, indicating the presence of beige cells. Further histological analyses of this fat depot confirmed the presence of beige adipocytes foci, characterized by the presence of multilocular lipid droplets in *LPTEN* KO (Fig. 4B).

The effect of hepatic *PTEN*-deficiency on muscle insulin sensitivity and fat storage in adipocytes highly suggests the presence of a crosstalk between the liver and peripheral organs. Liver-derived circulating factors, such as hepatokines and cytokines, play critical roles in these processes. We therefore assessed the expression of various factors secreted by the liver, and as shown in Fig. 4C, the expression of several hepatokines and cytokines, previously reported to modulate muscle insulin sensitivity and/or WAT homeostasis, was significantly affected in the liver of *LPTEN* KO mice. Of particular interest, was the fibroblast growth factor 21 (FGF21), which has a positive effect on muscle insulin sensitivity and browning of adipose tissue [22–25]. Expression of *Fgf21* was also strongly upregulated in isolated primary hepatocytes of *LPTEN* KO mice and plasma FGF21 levels mirrored the liver mRNA expression, altogether supporting a major hepatic origin of circulating FGF21 levels (Fig. 4D and E). However, depletion or overexpression of *PTEN* *per se* was not sufficient to affect *Fgf21* expression in primary hepatocytes isolated from CTL mice, while *PTEN* deletion in cultured human hepatoma cells (HuH-7) strongly stimulated *Fgf21* expression (Fig. 4F).

Altogether, these data indicate that hepatic *PTEN*-deficiency promotes a browning of specific WAT depots. The concerted action of several dysregulated liver-derived factors, including a significant upregulation of FGF21 production and secretion, is probably contributing to the crosstalk between metabolically stressed *PTEN*-deficient livers and skeletal muscle/adipose tissue,

triggering improved muscle insulin sensitivity and decreased adiposity.

Discussion

Alterations of inter-organ communications can lead to drastic phenotypical changes in the metabolic status of organisms. Herein, we demonstrate that impaired *PTEN* signalling in the liver leads to the development of NAFLD, while positively impacting on muscle and adipose tissue homeostasis, thereby improving systemic insulin sensitivity, glucose tolerance, and decreasing adiposity.

As previously reported, *LPTEN* KO mice develop a marked hepatic steatosis [16]. Based on our results, steatosis development arises not only from an increased *de novo* lipogenesis and decreased VLDL export as shown by Qiu *et al.* [26], but also from an increased FA uptake, as suggested by the significant upregulation of several FA transporters. This is linked with substantial changes in hepatic glucose metabolism, including enhanced glycolysis (whose products are essentially used for *de novo* lipogenesis), as well as decreased gluconeogenesis.

Given the increased liver glycolysis and inhibition of gluconeogenesis, hepatic-dependent sources of energy during starvation are likely restricted. Although kidneys and the gut may take over to maintain normoglycemia [27], other sources of energy might be provided by an increase in adipose tissue lipolysis, releasing FAs in the circulation. Such mechanisms might be responsible for the drastic reduction in adipose tissue depots of *LPTEN* KO mice. However, we do not favour this hypothesis since no significant difference in circulating NEFA levels was observed in *LPTEN* KO mice as compared to CTL mice and because the expression of key enzymes controlling adipocyte lipolysis was not significantly changed. Instead, inhibition of lipogenesis and FA esterification in WAT could partly explain the fat mass loss in *LPTEN* KO mice. Another mechanism may lie in the browning of white adipocytes (presence of beige cells), as detected by a significant upregulation of *Ucp1* and the presence of multilocular lipid droplets in the mesenteric WAT depot. Interestingly, the presence of beige adipocytes in WAT has been linked with improved glucose tolerance [28], which is precisely observed in *LPTEN* KO vs. CTL mice. This might be related to decreased gluconeogenesis, mentioned above, and/or to an increase in peripheral insulin sensitivity. With regard to the latter parameter, one of the key findings, arising from our analyses of insulin signalling in skeletal muscle and euglycemic-hyperinsulinemic clamps, was a marked enhancement of insulin sensitivity and resulting glucose uptake in skeletal muscles from *LPTEN* KO. This effect on muscles, together with the decreased adiposity, highly suggests the existence of a crosstalk between liver and muscle/adipose tissue. Supporting this hypothesis, we found an altered pattern of cytokines/hepatokines expression and/or secretion (e.g., IL-8, FGF21 and fetuin A) that were previously reported to mediate the crosstalk between liver and peripheral tissues and to have an action on muscle insulin sensitivity and adiposity [29]. Among them, FGF21 was overexpressed in the liver of *LPTEN* KO mice, resulting in elevated plasma FGF21 levels. This insulin-sensitizing hepatokine is of particular interest since it is known to enhance glucose uptake in muscle [22,23] and to increase energy expenditure in WAT [30]. Interestingly, FGF21 was also reported to stimulate UCP1 expression and browning of WAT [24,25], in accordance with our data. How *PTEN* controls FGF21 expression

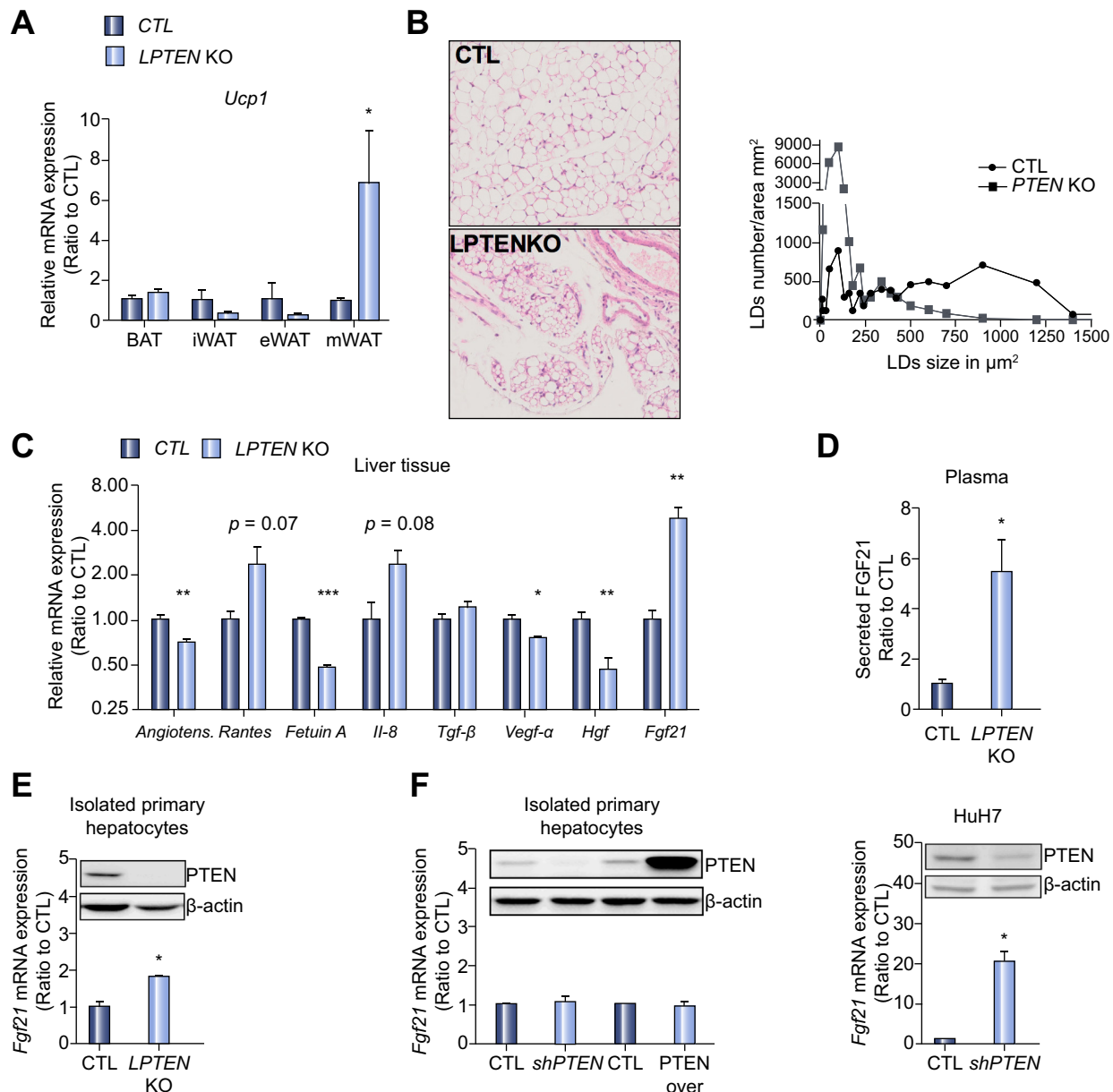


Fig. 4. Browning of WAT and increased hepatic FGF21 production in LPTEN KO mice. (A) *Ucp1* mRNA expression in white adipose tissue: iWAT, inguinal; eWAT, epididymal; mWAT, mesenteric, and in brown adipose tissue (BAT) depots. (B) mWAT sections stained with Haematoxylin/Eosin (magnification 10 \times). Quantification represents the number and area of lipid droplets per mm^2 of mWAT tissue section. (C) Relative mRNA expression of circulating liver-derived hepatokines and cytokines. (D) Plasma FGF21 levels. (E) PTEN protein expression and *Fgf21* mRNA expression in primary hepatocytes isolated from CTL and LPTEN KO mice. (F) PTEN protein expression and *Fgf21* mRNA expression in wild type primary hepatocytes transduced with lentiviral vectors expressing shPTEN, PTEN and respective control vectors (left panel) and HuH-7 hepatoma cells transduced with lentiviral vectors expressing shPTEN or a control vector (right panel). Values are mean \pm SEM of at least 4 animals per group or 3 independent experiments for cultured cells.

in hepatocytes remains currently unclear. AKT activation was previously reported to stimulate FGF21 expression in muscle [31], raising the possibility that FGF21 overexpression in the liver of LPTEN KO mice is a direct consequence of PTEN-dependent AKT over-activation. However, our data with primary hepatocytes, in which PTEN expression is either up- or downregulated, argue against this hypothesis, and suggest that other hepatic metabolic stress and/or injuries are the main trigger of FGF21 overexpression, as previously described in various conditions and tissues [32]. Future studies should also evaluate whether the beneficial

effects of hepatic PTEN deletion on muscles and WAT are related to the mere overproduction of FGF21 by the liver, or to a concerted action of several hepatic circulating factors, modulated by PTEN-deficient signalling in hepatocytes.

In addition to our study, PTEN overexpression in transgenic mice was recently shown to induce increased energy expenditure, hyperactive brown adipose tissues and reduced body fat accumulation [11,12]. It is therefore clear that chronic alterations of PTEN signalling in peripheral organs are correlated with adipose tissue plasticity. However, it is likely that alterations of

Research Article

PTEN signalling in specific organs exert distinct effects on adipose tissue biology, through either direct or indirect mechanisms that are currently not fully understood. A deep understanding of the role of PTEN in metabolically active tissues and of PTEN-dependent molecular mechanisms, mediating crosstalks between peripheral organs, would not only improve our general understanding of inter-organ communications, but would also allow envisaging new therapeutic options to treat IR and obesity.

Financial support

This work was supported by the Swiss National Science Foundation (grant N°310030-152618 and N°CRSII3-141798 to M. Foti and grant 31003A_134919/1 to F. Rohner-Jeanrenaud), the EFSD Research Programme in Diabetes and Cancer, The Swiss Cancer League (KFS-02502-08-2009), the Fondation Romande pour la Recherche sur le Diabète, the Desirée and Niels Yde Foundation to M. Foti and the EU FP7 project DIABAT (Health-F2-2011-278373) to F. Rohner-Jeanrenaud.

Conflict of interest

The authors who have taken part in this study declared that they do not have anything to disclose regarding funding or conflict of interest with respect to this manuscript.

Authors' contributions

M. Peyrou, L. Bourgoïn: study concept and design; acquisition, analysis and interpretation of data; drafting of the manuscript. A.-L. Poher, J. Altirriba, C. Maeder, A. Caillon, M. Fournier, X. Montet: acquisition, analysis and interpretation of data. F. Rohner-Jeanrenaud: analysis and interpretation of data; drafting of the manuscript; critical revision of the manuscript for important intellectual content; obtained funding. M. Foti: study concept and design; analysis and interpretation of data; drafting of the manuscript; critical revision of the manuscript for important intellectual content; obtained funding; study supervision.

Acknowledgement

We thank Christian Vesin for his help with mouse primary hepatocyte isolation.

Supplementary data

Supplementary data associated with this article can be found, in the online version, at <http://dx.doi.org/10.1016/j.jhep.2014.09.012>.

References

- Trauner M, Arrese M, Wagner M. Fatty liver and lipotoxicity. *Biochim Biophys Acta* 2010;1801:299–310.
- Loria P, Lonardo A, Anania F. Liver and diabetes. A vicious circle. *Hepatology* 2013;43:51–64.
- Nolan CJ, Damm P, Prentki M. Type 2 diabetes across generations: from pathophysiology to prevention and management. *Lancet* 2011;378:169–181.
- Milic S, Stimac D. Nonalcoholic fatty liver disease/steatohepatitis: epidemiology, pathogenesis, clinical presentation and treatment. *Dig Dis* 2012;30:158–162.
- Maehama T, Dixon JE. The tumor suppressor, PTEN/MMAC1, dephosphorylates the lipid second messenger, phosphatidylinositol 3,4,5-trisphosphate. *J Biol Chem* 1998;273:13375–13378.
- Salmena L, Carracedo A, Pandolfi PP. Tenets of PTEN tumor suppression. *Cell* 2008;133:403–414.
- Shen WH, Balajee AS, Wang J, Wu H, Eng C, Pandolfi PP, et al. Essential role for nuclear PTEN in maintaining chromosomal integrity. *Cell* 2007;128:157–170.
- Kurlawalla-Martinez C, Stiles B, Wang Y, Devaskar SU, Kahn BB, Wu H. Insulin hypersensitivity and resistance to streptozotocin-induced diabetes in mice lacking PTEN in adipose tissue. *Mol Cell Biol* 2005;25:2498–2510.
- Wijesekara N, Konrad D, Eweida M, Jefferies C, Liadis N, Giacca A, et al. Muscle-specific Pten deletion protects against insulin resistance and diabetes. *Mol Cell Biol* 2005;25:1135–1145.
- Wong JT, Kim PT, Peacock JW, Yau TY, Mui AL, Chung SW, et al. Pten (phosphatase and tensin homologue gene) haploinsufficiency promotes insulin hypersensitivity. *Diabetologia* 2007;50:395–403.
- Garcia-Cao I, Song MS, Hobbs RM, Laurent G, Giorgi C, de Boer VC, et al. Systemic elevation of PTEN induces a tumor-suppressive metabolic state. *Cell* 2012;149:49–62.
- Ortega-Molina A, Efeyan A, Lopez-Guadamillas E, Munoz-Martin M, Gomez-Lopez G, Canamero M, et al. Pten positively regulates brown adipose function, energy expenditure, and longevity. *Cell Metab* 2012;15:382–394.
- Vinciguerra M, Veyrat-Durebex C, Moukil MA, Rubbia-Brandt L, Rohner-Jeanrenaud F, Foti M. PTEN down-regulation by unsaturated fatty acids triggers hepatic steatosis via an NF-kappaBp65/mTOR-dependent mechanism. *Gastroenterology* 2008;134:268–280.
- Clement S, Peyrou M, Sanchez-Pareja A, Bourgoïn L, Ramadori P, Suter D, et al. Down-regulation of phosphatase and tensin homologue by hepatitis C virus core 3a in hepatocytes triggers the formation of large lipid droplets. *Hepatology* 2011;54:38–49.
- Horie Y, Suzuki A, Kataoka E, Sasaki T, Hamada K, Sasaki J, et al. Hepatocyte-specific Pten deficiency results in steatohepatitis and hepatocellular carcinomas. *J Clin Invest* 2004;113:1774–1783.
- Stiles B, Wang Y, Stahl A, Bassilian S, Lee WP, Kim YJ, et al. Liver-specific deletion of negative regulator Pten results in fatty liver and insulin hypersensitivity. *Proc Natl Acad Sci U S A* 2004;101:2082–2087.
- Bruss MD, Khambatta CF, Ruby MA, Aggarwal I, Hellerstein MK. Calorie restriction increases fatty acid synthesis and whole body fat oxidation rates. *Am J Physiol Endocrinol Metab* 2010;298:E108–E116.
- Bouskila M, Hirshman MF, Jensen J, Goodyear LJ, Sakamoto K. Insulin promotes glycogen synthesis in the absence of GSK3 phosphorylation in skeletal muscle. *Am J Physiol Endocrinol Metab* 2008;294:E28–E35.
- Vettor R, Cusin I, Ganten D, Rohner-Jeanrenaud F, Ferrannini E, Jeanrenaud B. Insulin resistance and hypertension: studies in transgenic hypertensive TGR(mREN-2)27 rats. *Am J Physiol* 1994;267:R1503–R1509.
- Peyrou M, Bourgoïn L, Foti M. PTEN in non-alcoholic fatty liver disease/non-alcoholic steatohepatitis and cancer. *Dig Dis* 2010;28:236–246.
- Bartelt A, Heeren J. Adipose tissue browning and metabolic health. *Nat Rev Endocrinol* 2014;10:24–36.
- Camporez JP, Jornayvaz FR, Petersen M, Pesta D, Guigni BA, Serr J, et al. Cellular mechanisms by which FGF21 improves insulin sensitivity in male mice. *Endocrinology* 2013;154(9):3099–3109.
- Mashili FL, Austin RL, Deshmukh AS, Fritz T, Caidahl K, Bergdahl K, et al. Direct effects of FGF21 on glucose uptake in human skeletal muscle: implications for type 2 diabetes and obesity. *Diabetes Metab Res Rev* 2011;27:286–297.
- Fisher FM, Kleiner S, Douris N, Fox EC, Mepani RJ, Verdeguer F, et al. FGF21 regulates PGC-1alpha and browning of white adipose tissues in adaptive thermogenesis. *Genes Dev* 2012;26:271–281.
- Emanuelli B, Vienberg SG, Smyth G, Cheng C, Stanford KI, Arumugam M, et al. Interplay between FGF21 and insulin action in the liver regulates metabolism. *J Clin Invest* 2014;124:515–527.
- Qiu W, Federico L, Naples M, Avramoglu RK, Meshkani R, Zhang J, et al. Phosphatase and tensin homolog (PTEN) regulates hepatic lipogenesis, microsomal triglyceride transfer protein, and the secretion of apolipoprotein B-containing lipoproteins. *Hepatology* 2008;48:1799–1809.

- [27] Mithieux G, Gautier-Stein A, Rajas F, Zitoun C. Contribution of intestine and kidney to glucose fluxes in different nutritional states in rat. *Comp Biochem Physiol B Biochem Mol Biol* 2006;143:195–200.
- [28] Seale P, Conroe HM, Estall J, Kajimura S, Frontini A, Ishibashi J, et al. Prdm16 determines the thermogenic program of subcutaneous white adipose tissue in mice. *J Clin Invest* 2011;121:96–105.
- [29] Stefan N, Haring HU. The role of hepatokines in metabolism. *Nat Rev Endocrinol* 2013;9:144–152.
- [30] Chau MD, Gao J, Yang Q, Wu Z, Gromada J. Fibroblast growth factor 21 regulates energy metabolism by activating the AMPK-SIRT1-PGC-1alpha pathway. *Proc Natl Acad Sci U S A* 2010;107:12553–12558.
- [31] Izumiya Y, Bina HA, Ouchi N, Akasaki Y, Kharitonov A, Walsh K. FGF21 is an Akt-regulated myokine. *FEBS Lett* 2008;582:3805–3810.
- [32] Luo Y, McKeenan WL. Stressed liver and muscle call on adipocytes with FGF21. *Front Endocrinol (Lausanne)* 2013;4:194.